Ideal linear-chain polymers with fixed angular momentum

Matthew Brunner and J. M. Deutsch
Department of Physics, University of California Santa Cruz, Santa Cruz, California 95064, USA
(Received 25 August 2010; published 15 July 2011)

The statistical mechanics of a linear noninteracting polymer chain with a large number of monomers is considered with fixed angular momentum. The radius of gyration for a linear polymer is derived exactly by functional integration. This result is then compared to simulations done with a large number of noninteracting rigid links at fixed angular momentum. The simulation agrees with the theory up to finite-size corrections. The simulations are also used to investigate the anisotropic nature of a spinning polymer. We find universal scaling of the polymer size along the direction of the angular momentum, as a function of rescaled angular momentum.

DOI: 10.1103/PhysRevE.84.011804 PACS number(s): 82.35.Lr

I. INTRODUCTION

Polymer chains in a vacuum have been shown to have great importance in many experimental situations, most often in application to mass spectroscopy techniques that utilize the desorption of proteins into a vacuum. The ability to desorb very large molecules without compromising their integrity has many uses in biology [1]. Understanding the statistical mechanics of such systems may help to improve current spectroscopic techniques by providing information about other quantities, aside from mass, that may be usefully measured. Aside from other applications [2], there is also the intrinsic interest in understanding such systems.

The dynamics of vacuum polymers have been the subject of a number of recent investigations [2–7] and show many unusual features that are different from those seen in solution. Polymers close to the coil-globule transition show small Lyapunov exponents [4]. However, in many situations, the dynamics are in accord with detailed microcanonical calculations, implying that these systems are ergodic [6]. Ideal chains show highly oscillatory time correlation functions [2], whereas the addition of self-interactions damps these oscillations, although they are still quite pronounced for small chains [6]. Although there is no coupling to a heat bath, the nonlinear dynamics of these models give rise to an effective damping of individual monomers that is similar to that of Kelvin damping [8]. Adding local angular potentials to polymers increases this type of damping but does not inhibit oscillations for sufficiently long chains [5].

In this paper we investigate the equilibrium statistics of a noninteracting polymer chain of N links in a vacuum, where energy, momentum, and angular momentum are conserved. Previous work [7] found an analytical solution for a ring polymer with conserved angular momentum. The average radius of gyration as a function of angular momentum was obtained. The most surprising feature of that calculation is that the radius of gyration when the angular momentum is zero is less than that of a chain without that conservation law. The radius of gyration is still proportional to $\sqrt{N}$ but now with a different proportionality constant.

The calculation performed for a ring chain [7] does not extend easily to linear chains. Here we use an approach that diverges considerably from the previous one to obtain the statistics of a linear chain under the same conditions. The present approach has some similarities to techniques used in statistical quantum mechanics [9]. In both cases, although the intermediate steps produce rather lengthy expressions, the final answers are quite simple. This suggests that there may be another underlying principle that can be used to understand systems with constant angular momentum.

Aside from the average radius of gyration of such a system, there is another important quantity that describes it. For finite angular momentum, the chain is expected to become anisotropic, flattening in the direction of the angular momentum vector. It is therefore of interest to calculate the average size of a chain both perpendicular and parallel to the angular momentum. However, our analytic method is only applicable in calculating quantities that have rotational symmetry such as the radius of gyration. It will not work for studying chain anisotropy. Therefore we turn to numerical methods to study this problem. We find, rather surprisingly, that the chain continuously flattens in the direction of the angular momentum showing universal scaling in the same rescaled variables used to characterize the full radius of gyration.

II. EXACT SOLUTION

Following previous work [10], we begin by writing down the entropy as a function of the total energy E, angular momentum L, and number of particles N, including terms for the conservation laws to be enforced:

$$W(E,L,N) = C \int \delta(E-K-\Phi)\delta^{(3)}\left(\mathbf{L} - \sum_i \mathbf{r}_i \times \mathbf{p}_i\right)\delta^{(3)} \times (\mathbf{r}_{\text{c.m.}})\left(\prod_{i=1}^{N} d^3 r_i d^3 p_i\right), \quad (1)$$

where K is the total kinetic energy and Φ is the total potential energy. We are choosing a coordinate system so that the center of mass $\mathbf{r}_{\text{c.m.}} = 0$.

We take the potential energy to be the elastic energy of the polymer chain and in addition include an isotropic quadratic potential that will be used to calculate the radius of gyration. In terms of the continuous arc-length s-dependent position variables that we will use below,

$$\beta\Phi = \int_0^{Nl} \frac{3}{2l}\left|\frac{d\mathbf{r}}{ds}\right|^2 + \epsilon r^2(s) ds, \quad (2)$$

where l is the chain link length, which is independent of the other properties of the chain. Because we are taking N to be large, we can convert this to a partition function, with the energy-conserving δ function expanded in exponential form:

$$Z(\beta,L,N) \propto \int d^3k \int e^{i\mathbf{k}\cdot\mathbf{L}} e^{-\beta(K+\Phi)} \exp\left(-i\mathbf{k}\cdot\sum_i \mathbf{r}_i \times \mathbf{p}_i\right) \times \delta^{(3)}(\mathbf{r}_{\text{c.m.}}) \left(\prod_{i=1}^{N} d^3 r_i d^3 p_i\right). \quad (3)$$

After integrating over the momenta and taking into account rotational symmetry we arrive at the form [7]

$$Z[\beta,L,N] = \frac{c}{L}\int_0^\infty \sin(kL)\zeta(\beta,k)dk, \quad (4)$$

where ζ is a function of the magnitude of k and inverse temperature β only. The constant c is of no physical importance and

$$\zeta(\beta,k) = \int \exp\left[-\int_0^{Nl}\left(\frac{Tmk^2}{2l}+\epsilon\right)[x(s)^2+y(s)^2] + \epsilon z(s)^2 + \frac{3}{2l}|\dot{\mathbf{r}}|^2 ds\right]\delta(\mathbf{r}_{\text{c.m.}})\delta\mathbf{r}(s). \quad (5)$$

Now we perform a scaling on L, k, and s in order to normalize out the length of the chain and the temperature:

$$L' = \frac{\sqrt{12}}{Nl\sqrt{mT}}L, \quad (6)$$

$$k' = \frac{Nl\sqrt{mT}}{\sqrt{12}}k, \quad (7)$$

$$s' = \frac{\sqrt{12}}{Nl}s. \quad (8)$$

The rescaling factors are based on the expected value of L for the usual model without conservation of angular momentum and produce a set of dimensionless variables. This will allow us to compare chains of all sizes and temperatures on a common scale. After doing these rescalings, the form of Eq. (4) remains unchanged and Eq. (5) changes to

$$\zeta(\beta,k') = \int \exp\left(-\int_0^{\sqrt{12}}(k'^2/2l+\epsilon')[x'(s')^2+y'(s')^2] + \epsilon' z'(s')^2 + \frac{3}{2l}|\dot{\mathbf{r}}'|^2 ds'\right)\delta\left(\mathbf{r}'_{\text{c.m.}}\right)\delta\mathbf{r}'(s'). \quad (9)$$

It is interesting to note that the explicit dependence on β has disappeared and ζ is now only a function of k'. The dependence on the total length of the chain has also been factored into k', but the length of the individual monomers remains. Now we expand the center-of-mass-conserving δ function in a complex exponential form

$$\zeta(k') = \int \exp\left(-\int_0^{\sqrt{12}}(k'^2/2l+\epsilon')(x'^2+y'^2)+\epsilon' z'^2 + \frac{3}{2l}|\dot{\mathbf{r}}'|^2 + ix'l_x + iy'l_y + iz'l_z ds'\right) dl_x dl_y dl_z \delta\mathbf{r}'(s'). \quad (10)$$

These terms can be combined with the existing exponents using a completion of squares, which results in path-independent phase factors and a constant offset to the paths, e.g., $x'(s) \to x'(s) + \text{const}$. Since all possible paths are included in the integral, the offset has no effect.

We now have a nice separation into a simple Gaussian integral and a factor that is very similar to the path-integral form of a harmonic oscillator:

$$\left(\int \exp\left\{\sqrt{12}\left[-(l_x^2+l_y^2)/4\left(\frac{k'^2}{2l}+\epsilon'\right)-l_z^2/4\epsilon'\right]\right\} \times dl_x dl_y dl_z\right)\left[\int \exp\left(-\int_0^{\sqrt{12}}(k'^2/2l+\epsilon')(x'^2+y'^2) + \epsilon' z'^2 + \frac{3}{2l}|\dot{\mathbf{r}}'|^2\right)\delta\mathbf{r}'\right]. \quad (11)$$

The first integrals of the l's are trivially integrated, but we must still perform the path integral in large parentheses. These decouple into path integrals over the x, y, and z directions and each one has an action of the form

$$\int_0^{\beta_0}\frac{M}{2}(\dot{x}^2+\omega_0^2 x^2)dt. \quad (12)$$

M does not depend on k or ϵ, and ω_z has no k dependence. After making this analogy, we can see that for any two fixed-path end points, the functional integration will give the Green's function for a thermal harmonic oscillator. To obtain a sum over all paths, we simply need to integrate the Green's function ρ [11] over both its arguments,

$$\zeta_i = \int \rho_i(x_1,x_2)dx_1 dx_2, \quad (13)$$

where $i = 1$, 2, and 3 represent the x, y, and z, path integrals, respectively. The Green's function is easily integrated and the result is

$$\zeta_i \propto \frac{\omega_i}{\sqrt{\sinh(\sqrt{12}\omega_i)}}. \quad (14)$$

Putting all of this back into Eq. (4), we get the form for Z,

$$Z(L') = \frac{c}{L}\sqrt{\frac{\omega_z}{\sinh(\sqrt{12}\omega_z)}}\int_0^\infty k' \sin(k'L')\frac{\omega}{\sinh(\sqrt{12}\omega)}dk'. \quad (15)$$

The radius of gyration can be expressed as

$$R_g^2 = -\frac{1}{Nl}\frac{\partial \ln Z}{\partial\epsilon}\bigg|_{\epsilon=0}. \quad (16)$$

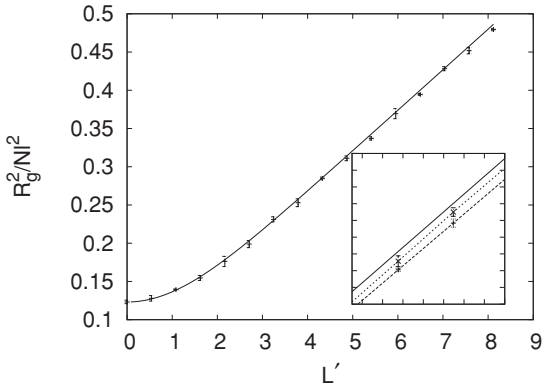

FIG. 1. Plot of $\frac{R_g^2}{Nl^2}$ along with simulation results using a chain length $N = 128$. The inset is a section from $L' = 5.5$ to 7 showing the exact solution as a solid line along with results from simulations done with $N = 32$ (farthest from line) and $N = 64$.

The logarithmic derivative allows us to separate the factors in Z and treat each as terms in a sum. The first term is simple:

$$\lim_{\epsilon\to 0}\frac{\partial \ln}{\partial \epsilon}\sqrt{\frac{\omega_z}{\sinh(\sqrt{12}\omega_z)}} = -\frac{1}{18}N^2l^3. \tag{17}$$

The second term is more complex due to the integral, so we begin by rewriting the logarithmic derivative as a ratio:

$$\lim_{\epsilon\to 0}\frac{\frac{\partial}{\partial\epsilon}\int_0^\infty k'\sin(k'L')\frac{\omega}{\sinh(\sqrt{12}\omega)}dk'}{\int_0^\infty k'\sin(k'L')\frac{\omega}{\sinh(\sqrt{12}\omega)}dk'}. \tag{18}$$

Since the integral is over k' we can pull the derivative and limit inside the integration. This simplifies the integrand considerably as $\lim_{\epsilon\to 0}\omega = k'/\sqrt{3}$:

$$\lim_{\epsilon\to 0}\frac{\frac{\partial}{\partial\epsilon}\int_0^\infty k'\sin(k'L')\frac{\omega}{\sinh(\sqrt{12}\omega)}dk'}{\int_0^\infty k'\sin(k'L')\frac{\omega}{\sinh(\sqrt{12}\omega)}dk'} = \frac{L'N^2}{6\pi l^3\tanh\left(\frac{L'\pi}{4}\right)}. \tag{19}$$

Putting all of these pieces together we obtain our final result,

$$\frac{R_g^2}{Nl^2} = \frac{1}{18} + \frac{L'}{6\pi\tanh\left(\frac{L'\pi}{4}\right)}. \tag{20}$$

A plot of this is shown in Fig. 1 by the solid line. The simulation results that are also displayed will be discussed in Sec. V. Note that for $L' = 0$, $R_g^2/Nl^2 = 1/18 + 2/3\pi^2 \approx 0.1231$, which is about 74% of $1/6$, the value of the same quantity without conservation of angular momentum enforced. For the same reason as for the ring calculation [7], for fixed L' and $N \to \infty$, we are permitted to take this system to be at constant temperature because, as discussed in detail [7], the relation between energy and temperature has no dependence on L' in this limit.

III. HIGH-L LIMIT

In the limit of large L, Eq. (20) gives $R_g^2/Nl^2 \to L'/6\pi$. One would expect that typical configurations at high L would consist of a fairly straight line rotating rapidly around its center. The solution for the equilibrium case of constant angular velocity can be found by setting the change in tension along the chain equal to the centripetal force. This gives an equation for the position of each monomer as a function of its location along the chain $r(s)$, for simplicity defined with $s = 0$ at the center of the chain. For large N, the tension approaches zero at the ends of the chain,

$$-k\frac{d^2r}{ds^2} = m\omega^2 r, \tag{21}$$

where k is the entropic elastic spring coefficient. From this we get that $r(s) \propto \sin(\sqrt{\frac{m}{k}}\omega s)$ and $Nl\omega/2\sqrt{k} = \pi/2$. Higher modes exist, but they double back and are expected to not be minimal free-energy solutions. They are also not consistent with the straight chain model we are assuming. Using the integral definition of angular momentum

$$L = \frac{m\omega}{l}\int_0^{Nl} r^2(s)ds, \tag{22}$$

the radius of gyration squared is

$$R_g^2 \equiv \frac{1}{Nl}\int r^2(s)ds = \frac{1}{\omega mN}L = \frac{1}{\sqrt{mk}\pi}L = \frac{l}{\sqrt{3mT}\pi}$$
$$L = \frac{L'Nl^2}{6\pi} \tag{23}$$

and therefore we see that in the limit of high L, our model behaves as one would expect.

IV. PARTITION FUNCTION

The partition function itself can be obtained easily from Eq. (14) by taking $\epsilon \to 0$ and performing the integration

$$\lim_{\epsilon\to 0} Z = \frac{1}{L}\int k'^2\frac{\sin(k'L')}{\sinh(2k')}dk' = \frac{\pi^3}{32L'}\frac{\tanh(L'\frac{\pi}{4})}{\cosh^2(L'\frac{\pi}{4})}. \tag{24}$$

To obtain the distribution over L' we need to normalize this Z, taking into account the angular integration over the direction of L',

$$\int 4\pi L'^2 Z dL' = \pi^2, \tag{25}$$

so our normalized partition function is

$$Z = \frac{\pi}{32L'}\frac{\tanh(L'\frac{\pi}{4})}{\cosh^2(L'\frac{\pi}{4})}. \tag{26}$$

A plot of this is displayed in Fig. 2. This partition function can be related to the probability density in the space of angular momentum. Since Z was normalized for three dimensions, it will be the three-dimensional density $\rho(\mathbf{L}')d\mathbf{L}'$. One can simply integrate out the trivial angular dimensions to get the density in terms of the radial scalar L'. The distribution shows a long exponential tail into high L'.

V. SIMULATION RESULTS

In addition to the exact calculation, further studies were carried out using simulation. First the analytical results concerning the radius of gyration as a function of L' were verified. Second we were able to investigate other quantities that were beyond the means of our analytic method.

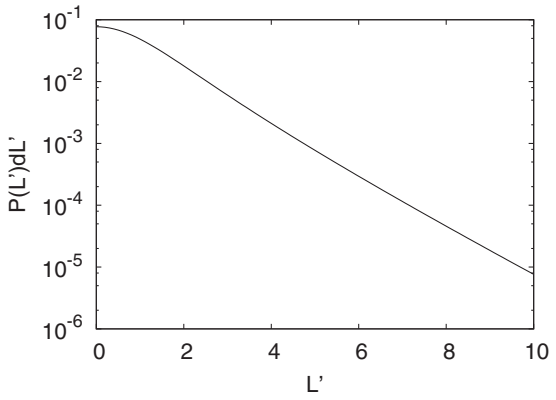

FIG. 2. Plot of $P(L')$, with clear non-Gaussian behavior for high L'.

We used a molecular-dynamics method [5] that was developed to simulate chains in a vacuum. It consisted of freely rotating rigid links, conserving energy and angular momentum, corresponding to a system with fixed temperature and angular momentum. Rigid links were employed to minimize problems with equilibration that are often seen with one-dimensional nonlinear systems [12,13]. The input angular momentum and the output measurements were scaled by the total chain length for comparison. The initial values of the angular momentum were chosen to cover a range of L' values and the angular momentum was explicitly checked and conserved during the runs. First the simulation was compared to the theoretical results for the normalized radius of gyration. The results of these simulations can be seen in Fig. 1 and show excellent agreement with the theoretical prediction. The main plot shows the exact result (solid line) along with data for chains with $N = 128$. The inset shows that the deviation in the asymptotic form for high L' decreases as the number of simulation chain links is increased and appears to be due to the finite size of the simulation system. The two chains lengths used in the inset are $N = 32$ and 64, which are more accurate than the data for $N = 128$. They also indicate that the finite-size corrections to the analytic form are $O(1/N^{\alpha})$ for some α of order unity, as shown in Fig. 3.

For nonzero angular momentum the polymer chain is expected to become anisotropic. The analytic methods used

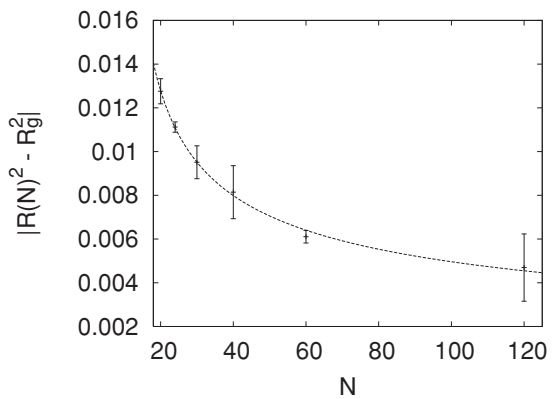

FIG. 3. Plot of the deviations in R_g^2 as a function of chain size N. The dashed line is the best-fit curve with $\alpha = 0.436$.

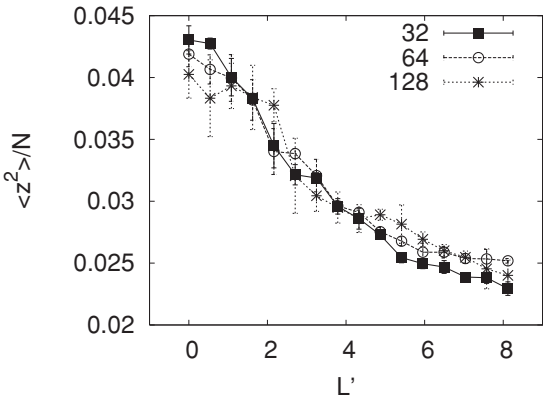

FIG. 4. Plot of the simulated radius of gyration in the direction of angular momentum as a function of rescaled L, for chain sizes $N = 32$, 64, and 128.

earlier require an isotropic form for the quantities being averaged, causing the investigation of the anisotropy by such means to be outside the scope of our analysis. Therefore, we turned to the simulation to explore the aspect ratio of the polymer as a function of L', with the aspect ratio defined as $\sqrt{\langle z^2\rangle/\langle R_g^2\rangle}$. The aspect ratio itself is dominated by the asymptotic linear behavior of the radius of gyration and displays what appears to be an inverse power-law falloff as expected. More interestingly, $\langle z^2\rangle$ itself appears to fall off as L' increases, even for low values of L'. This is shown in Fig. 4, where the vertical axis is scaled in the same manner as for the radius of gyration, by dividing by N and taking l, m, and T all to be unity, and the horizontal axis is L'. The three chain lengths seem to collapse onto one curve after the rescaling of length and angular momentum. This is unexpected because for an ideal Gaussian chain each dimension has independent statistics, which our model should resemble for low R_g. The coupling should only be apparent in the limit of high L, where the rigid link model should approach a straight-line solution. However, this is unlikely to be an explanation, as the straight-line regime would imply a leveling off of the radius of gyration, which is not seen (see Fig. 1). Moreover, the falloff is independent of the number of chain links in the simulation and collapsed onto a single curve, so is not likely due to the non-Gaussian nature of the model. This decrease in $\langle z^2\rangle$ is slow, does not appear to have a nonzero asymptote, and is likely to be a low power law or logarithmic in nature.

VI. CONCLUSION

In this paper we considered the equilibrium properties of an ideal linear chain in a vacuum that conserves energy, momentum, and angular momentum. We were able to compute the average radius of gyration of such a chain as a function of its angular momentum L. We also computed the distribution of angular momenta for chains in thermal equilibrium. We verified that our analytical result for the radius of gyration is correct by performing numerical simulations and by analyzing its asymptotic form in the limit of large angular momentum. The derivation of this result differs from that of a ring chain, but in both cases the final result is relatively simple involving

hyperbolic trigonometric functions. The underlying reason for this is still unclear.

Our numerical simulations show that the radius of gyration perpendicular to the angular momentum vector increases with L, as to be expected; however, in addition to this, the radius of gyration parallel to the angular momentum, which we take to be in the z direction, decreases. This is very different from what a naive analysis would suggest. If we were to go to a frame rotating at angular velocity Ω, then in thermal equilibrium (without angular momentum conservation), this is equivalent to an additional potential $-m\Omega^2 r_{xy}^2/2$, where r_{xy} is the projection of a coordinate onto the x-y plane. For an ideal Gaussian chain, all three directions decouple and $\langle z^2 \rangle$ is independent of L. However, a more rigorous analysis based on the approach of this paper is not equivalent to this and it is not clear how statistics in the x-y plane and z direction are coupled to cause this effect.

[1] *MALDI MS: A Practical Guide to Instrumentation, Methods and Applications*, edited by F. Hillenkamp and J. Peter-Katalinic (Wiley-VCH, Weinheim, 2007).

[2] J. M. Deutsch, Phys. Rev. Lett. **99**, 238301 (2007).

[3] H. Kleinert, Phys. Rev. B **76**, 052202 (2007).

[4] A. Mossa, M. Pettini, and C. Clementi, Phys. Rev. E **74**, 041805 (2006).

[5] J. M. Deutsch, Phys. Rev. E **81**, 061804 (2010).

[6] M. P. Taylor, K. Isik, and J. Luettmer-Strathmann, Phys. Rev. E **78**, 051805 (2008).

[7] J. M. Deutsch, Phys. Rev. E **77**, 051804 (2008).

[8] J. P. Sethna (unpublished).

[9] H. Kleinert, *Path Integrals in Quantum Mechanics, Statistics, Polymer Physics, and Financial Markets* (World Scientific, Singapore, 2006).

[10] V. Laliena, Phys. Rev. E **59**, 4786 (1999).

[11] Richard P. Feynman, *Statistical Mechanics: A Set of Lectures*, 2nd ed. (Westview, Boulder, 1998).

[12] E. Fermi, J. Pasta, and S. Ulam, Los Alamos National Laboratory Report No. LA-1940, 1955 (unpublished).

[13] For a review see G. P. Berman and F. M. Izrailev, Chaos **15**, 015104 (2005).